[Reprinted from the Journal of Physical Chemistry, 74, 2611 (1970).]
Copyright 1970 by the American Chemical Society and reprinted by permission of the copyright owner.

Kinetics of the Gas-Phase Pyrolysis of Poly(difluoramino)fluoromethanes[1]

by J. M. Sullivan, A. E. Axworthy, and T. J. Houser[2]

Rocketdyne, Division of North American Rockwell Corporation, Canoga Park, California *(Received November 14, 1969)*

The gas-phase thermal decompositions of tetrakis(difluoramino)methane, $C(NF_2)_4$, tris(difluoramino)fluoromethane, $FC(NF_2)_3$, and bis(difluoramino)difluoromethane, $F_2C(NF_2)_2$, were investigated over the temperature range 190–460° in stirred flow, tubular, and static reactors. The reactions are first-order, nonchain processes with C–N bond rupture as the rate-determining step in each case. The rate constants are given by the Arrhenius expressions: $C(NF_2)_4$, $k = 10^{16.14} \exp(-40{,}400/RT)$ sec^{-1}; $FC(NF_2)_3$, $k = 10^{16.45} \exp(-48{,}300/RT)$ sec^{-1}; $F_2C(NF_2)_2$, $k = 10^{15.75} \exp(-53{,}600/RT)$ sec^{-1}. The activation energies give a measurement of the bond dissociation energies for the first C–N bond in each molecule. All three compounds appear to decompose directly to NF_2, F, and the corresponding C=NF compound [*i.e.*, $(NF_2)_2C{=}NF$, $F(NF_2)C{=}NF$, and $F_2C{=}NF$, respectively]. Some of the $N_2F_4(NF_2)$ is converted into NF_3 *via* reaction with F atoms. The stable products (N_2, CF_4, NF_3, and CF_3NF_2) are formed from reactions of the C=NF intermediates. Fluorine atom abstraction reactions are shown not to occur. This explains the nonchain character of these decompositions.

Introduction

Recently, considerable kinetic data have become available on the thermal decomposition of perhalogenated polynitroalkanes both in the liquid and gas phases.[3–8] The decompositions of these polynitro compounds are first order with activation energies from 35 to 48 kcal/mol and unusually high Arrhenius A factors of $10^{15.5}$ to $10^{18.5}$ sec^{-1}. In general, the initial and rate-determining step is considered to be the rupture of a C–NO_2 bond[5] as postulated by Sullivan and Axworthy.[4]

$$RNO_2 \longrightarrow R\cdot + NO_2$$

The high A factors result from the reduced frequencies of the four rocking modes of R and NO_2 relative to the R–NO_2 axis in the transition state.[9]

We have investigated the gas-phase thermal decompositions of the series of poly(difluoramino)methanes—$C(NF_2)_4$, $FC(NF_2)_3$, and $F_2C(NF_2)_2$—using stirred flow, tubular, and static reactors. The rate parameters obtained are quite analogous to the polynitro compounds, again suggesting that the rate-determining step involves the simple cleavage of a C–N bond. By following the product distribution as a function of residence time, we were able to definitely establish that the initial step is C–N bond rupture and gain considerable insight into the processes occurring after the rate-determining step.

Apparatus and Experimental Techniques

Stirred Flow Reactor. A major portion of the data was obtained using a gas-phase, stirred flow reactor.[10,11] In this system the gas to be investigated is passed through a reactor that promotes complete mixing. Under conditions of steady flow, the system reaches a steady state in which the concentrations of the reactant gases and products are uniform throughout the reactor.

The compound to be investigated was contained in a 1.5-ft^3 stainless steel tank as an approximately 1% mixture with helium. The total pressure of the gases within the tank ranged from 30 to 100 psig. The flow rate was controlled using a Nupro fine metering valve. Additives were mixed with helium and introduced from an auxiliary tank.

The construction of the reactor is shown in Figure 1. The body of the reactor was a high-pressure, 90-ml monel bomb. The gases flowed into the center of the reactor through five 0.016-in. diameter orifices (four to the sides and one to the bottom). The reactor was heated electrically, and the temperature was measured with a chromel–alumel thermocouple mounted within the thermocouple well. The flow rate of the exit stream was measured with a soap bubble flow meter from which the gas was vented at atmospheric pressure.

The gases leaving the reactor were analyzed by gas chromatography. The chromatograph was a custom-

(1) This work was supported by the U. S. Air Force and the Advanced Research Projects Agency under Contracts No. AF04(611)-9380, AF04(611)-10544, and ARPA Order No. 24.

(2) Chemistry Department, Western Michigan University, Kalamazoo, Mich.

(3) H. P. Marshall, F. G. Borgardt, and P. Noble, Jr., *J. Phys. Chem.*, **69**, 25 (1965).

(4) J. M. Sullivan and A. E. Axworthy, *ibid.*, **70**, 3366 (1966).

(5) G. M. Nazin, G. B. Manelis, G. N. Nechiporenko, and F. I. Dubovitsky, *Combust. Flame*, **12**, 102 (1968).

(6) H. P. Marshall, F. B. Borgardt, and P. Noble, Jr., *J. Phys. Chem.*, **72**, 1513 (1968).

(7) G. M. Nazin, G. B. Manelis, and F. I. Dubovitsky, *Izv. Akad. Nauk SSSR Ser. Khim.* No. 11, 2631 (1968).

(8) G. M. Nazin, G. B. Manelis, and F. I. Dubovitsky, *ibid.*, No. 12, 2801 (1968).

(9) S. W. Benson, "Thermochemical Kinetics," John Wiley & Sons, Inc., New York, N. Y., 1968.

(10) K. G. Denbigh, *Trans. Faraday Soc.*, **40**, 352 (1944); **44**, 479 (1948); and B. Stead, F. M. Page, and K. G. Denbigh, *Discussions Faraday Soc.*, **2**, 263 (1947).

(11) W. C. Herndon, *J. Chem. Educ.*, **41**, 425 (1964).

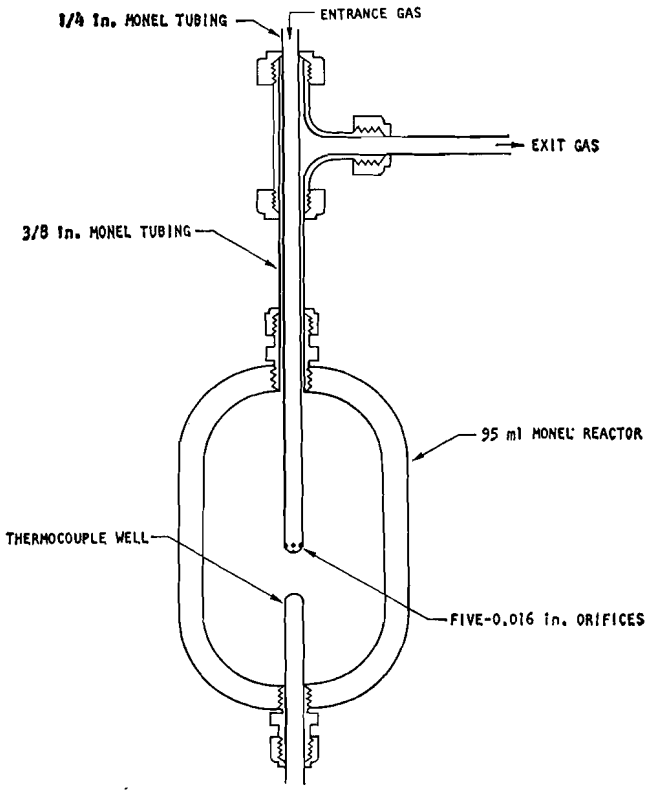


Figure 1. Stirred flow reactor.

built instrument, specifically designed to handle corrosive gases and employed a nickel thermal conductivity detector. Periodic sampling of the exit gas from the reactor, to determine reactant consumption and product formation, was accomplished with a Beckman 104176 gas-sampling valve connected directly between the reactor and the flow meter in the reactor exit stream. The reactor was equipped with a bypass to permit initial concentrations to be measured.

For a single-reactant, n-order reaction in a stirred flow reactor, the concentration of reactant at steady state is given by

$$dN/dt = C_0U - CU - k_nC^nV = 0 \qquad (1)$$

where N is the moles of reactant in the reactor, C_0 and C are the concentrations of reactant in the inlet stream and at the exit, respectively, U is the volume flow rate, V is the volume of the reactor, and k_n the specific rate constant. C_0, C, and U are corrected to reactor temperature. From eq 1

$$(C_0 - C)/C^n = k_n\tau \qquad (2)$$

where $\tau \equiv V/U$ is the average residence time in the reactor.

The utility of the stirred flow reactor is based on the assumption that there is complete mixing within the reactor. A series of experiments was conducted to test the validity of this assumption. If a few Torr of a stable tracer gas in 1 atm of helium is allowed to flow

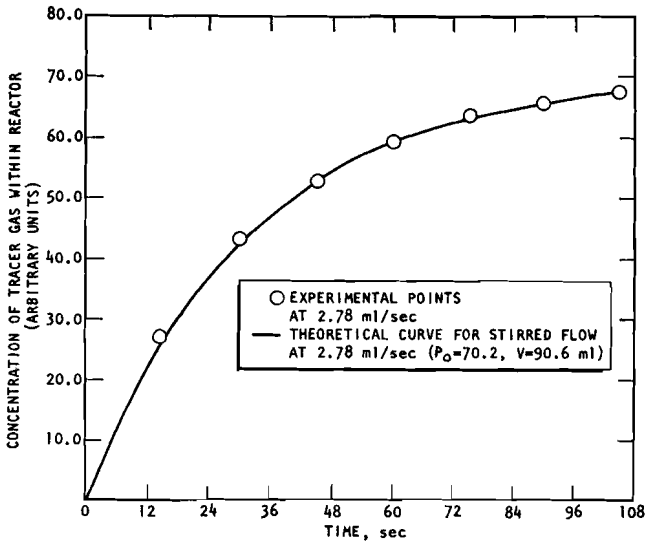


Figure 2. Approach to steady state in stirred flow reactor.

into a stirred flow reactor, which initially contains only helium, the partial pressure of the tracer gas should approach a steady state exponentially according to the equation

$$C = C_0(1 - e^{-t/\tau}) \qquad (3)$$

where the time, t, is measured from the initial response of the recorder. Equation 3 is obtained by integrating eq 1 for $dN/dt \neq 0$ and $k_n = 0$.

Mixing experiments were conducted at room temperature and 1 atm using $FC(NF_2)_3$ at 9 Torr as the tracer gas. The concentration of tracer gas leaving the reactor was monitored continuously by connecting the exit stream from the reactor directly to a thermal conductivity cell. Runs were made at flow rates of 0.29–9.9 ml/sec. In each case, the experimental values fit the theoretical concentrations given by eq 3. The results of a typical room temperature run at 2.78 ml/sec are shown in Figure 2. Experiments at 300° using nitrogen as the tracer gas at flowrates of 0.81–30.1 ml/sec are reported elsewhere[12] for this reactor. The results are again in agreement with eq 3.

Tubular Reactors. Two tubular reactors were employed to extend the range of experimental conditions investigated. The system was the same except that the stirred flow reactor was replaced by one of the tubular reactors.

The first tubular reactor consisted of 366 cm of $^1/_4$-in. monel tubing coiled to fit into a furnace. The internal diameter of the tubing was 0.180 in., and the volume of the heated reactor was 59.2 ml. The interior of the furnace was packed with aluminum foil to ensure even heating of the reactor. The temperature of the reactor was measured with three chromel–alumel

(12) J. M. Sullivan and T. J. Houser, *Chem. Ind.* (London), 1057 (1965).

thermocouples located at the top, center, and bottom of the coil, respectively. The three temperatures were found to agree within 0.7° at 300°. This reactor offered a convenient way of altering the surface-to-volume ratio to investigate the possible heterogeneity of the decomposition reactions. The surface-to-volume ratio of the 60-ml tubular reactor was approximately eight times that of the 90-ml stirred flow reactor.

The second tubular reactor was constructed from $^1/_8$-in. copper tubing. The length of the heated tube was 112 cm and the internal diameter was 0.165 cm; hence, the volume was 2.4 ml. This small reactor was used primarily to investigate the product distributions at much higher temperatures and shorter residence times (10–190 msec) than were obtainable in the larger reactors.

For tubular flow reactors under conditions of plug flow, the integrated rate expression for a first-order reaction is given by

$$k_1\tau = \ln (C_0/C) \quad (4)$$

Static Reactor. The static reactor consisted of a 160-ml monel bomb connected directly to a Beckman gas chromatographic sampling valve. Samples were taken by evacuating the 1.5-ml sample loop, expanding gases from the reactor into the loop, and rotating the loop into the carrier gas stream of the gas chromatograph. The stirred, constant-temperature bath contained Dow Corning 200 silicone fluid. The Teflon-coated reactor was similar except that it was coated internally with Teflon 851-204 (from aqueous solution) and baked at 250°.

Chemicals. Gaseous samples of $C(NF_2)_4$, $FC(NF_2)_3$, and $F_2C(NF_2)_2$ at purities of 96, 91, and 96%, respectively, were supplied by Minnesota Mining and Manufacturing Co. The impurities consisted primarily of air along with small quantities of decomposition products. Owing to the extreme tendency of these compounds to explode violently, no attempt at further purification was undertaken. However, as will be shown, the impurity contents of these samples are not critical since the decompositions proceed *via* nonchain processes, the rates of which are unaffected by decomposition products and a wide variety of additives.

Samples of $(NF_2)_2C{=}NF$, $F(NF_2)C{=}NF$, $F_2C{=}NF$, and CF_3NF_2 were generously supplied by the Minnesota Mining and Manufacturing Co. and were generally of 90–95% purity. Samples of CF_4, N_2, N_2F_4, NF_3, and the additives F_2, O_2, N_2O_4, and NO were obtained at the highest purities available and used without further purification.

Product Analysis. The products and intermediates of decomposition were identified by trapping them (using slush baths at various temperatures) and comparing their gas chromatographic, mass spectrometric, and infrared characteristics with those of known compounds.

Gas chromatography was the principal technique used to measure the concentrations of reactants, products, and intermediates. The chromatographic columns and conditions used for these analyses are shown in Table I.

Table I: Gas Chromatography Columns and Conditions

	Retention time, min					
Species	Column A[a] 45 ml/min[f]	85 ml/min	Column B[b] 45 ml/min	Column C[c] 60 ml/min	Column D[d] 60 ml/min	Column E[e] 60 ml/min
$C(NF_2)_4$	20	9				
$FC(NF_2)_3$	9					
$F_2C(NF_2)_2$			20	35.5		
$(NF_2)_2C{=}NF$	9					
$F(NF_2)C{=}NF$				31.8		
$F_2C{=}NF$				21.2		
CF_3NF_2				18.4		
N_2F_4				19.9		
N_2				↑	5.2	3.3
CF_4				15.0	0.8	9.8
NF_3				↓	16.3	11.2

[a] 7.5 ft of 30 wt % halocarbon oil on Chromasorb W (acid washed), 25°; products and intermediates gave composite peaks at 3 and 5 min, respectively, at carrier gas flow of 45 ml/min. [b] Column A plus 20 ft of 30 wt % perfluorotributylamine on Celite 345, 25°; products and intermediates gave composite peaks at 15 and 16 min, respectively. [c] 17 ft of 30 wt % halocarbon oil on Chromasorb W (acid washed) plus 40 ft of 30 wt % perfluorotributylamine on Celite 345, −22°; a peak for $FC(NF_2)_3$ was eluted after 1.5 hr but was too broad to be usable. [d] Linde 5A molecular sieve, 25°; CF_4 and NF_3 gave poorly shaped peaks that were not usable. [e] Activated Alumina, −22°. [f] Carrier gas flow rate.

Kinetics of Pyrolysis

Rates and Kinetic Parameters. The thermal decomposition rates of $C(NF_2)_4$, $FC(NF_2)_3$, and $F_2C(NF_2)_2$ were investigated over the temperature range 190–460° using the three types of reactors described, with most of the data being obtained with the stirred flow reactor. Each of these compounds was found to decompose by a first-order process.

The first-order rate constants were calculated from eq 2 and 4 for the stirred flow and tubular reactors, respectively. C_0 and C for each reactant are related to the integrated chromatographic peak areas, A_0 and A, by $C = F_iA$, where F_i is the calibration factor for that species.[13] Since F_i cancels from eq 2 and 4, no calibration is necessary to obtain first-order rate constants.

The first-order nature of the decompositions in the stirred flow reactor is demonstrated in Figure 3, which gives a plot of $(A_0 - A)/A$ *vs.* τ for $C(NF_2)_4$, $FC(NF_2)_3$, and $F_2C(NF_2)_2$ at 232, 338, and 398°, respectively. In

(13) Experiments were conducted to establish that F_i is constant for these compounds over the concentration ranges employed.

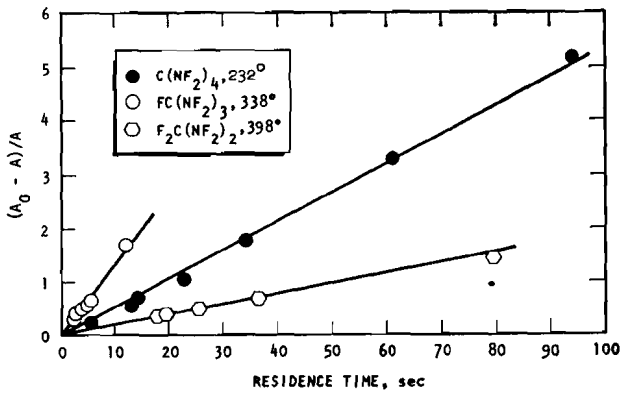


Figure 3. First-order plots.

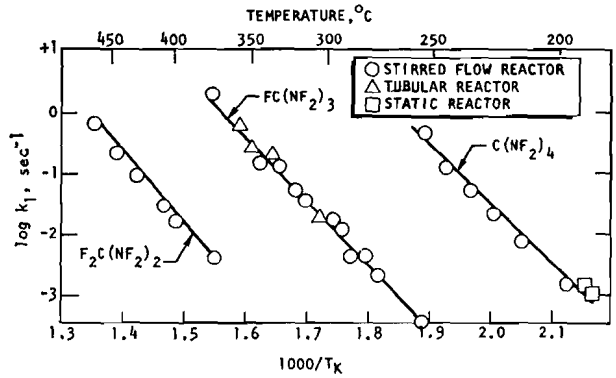


Figure 4. Arrhenius plots.

each case a straight line through the origin was obtained as predicted by eq 2. Significantly poorer fits were obtained for $n = {}^1/_2$ and $n = {}^3/_2$ in eq 2.

The experimental data and calculated first-order rate constants are available elsewhere.[14] The average rate constants obtained at each temperature are shown in the Arrhenius plots of Figure 4. $C(NF_2)_4$ was investigated over the temperature range 189.5–254.3°. The rate constants at 189.5 and 191.5° were obtained using the uncoated and Teflon-coated static reactors, respectively. The remainder of the rate constants for $C(NF_2)_4$ in Figure 4 were obtained with the stirred flow reactor. The rate constants for $FC(NF_2)_3$ over the temperature range 253–377°, obtained with the 90-ml stirred flow reactor and the 60-ml tubular reactor, are also plotted in Figure 4. The rates are in quite good agreement despite the fact the tubular reactor had a surface-to-volume ratio, S/V, approximately eight times that of the stirred flow reactor. The first-order rate constants for the decomposition of $F_2C(NF_2)_2$ in the stirred flow reactor (Figure 4) were obtained over the temperature range 372–457°.

The Arrhenius parameters for the decomposition of $C(NF_2)_4$, $FC(NF_2)_3$, and $F_2C(NF_2)_2$ are presented in Table II. These were obtained by least-squares fits of the flow reactor data to the Arrhenius expression.

Table II: Arrhenius Parameters

Compound	Log A	E, cal/mol
$C(NF_2)_4$	16.14 ± 0.17	40,400 ± 400
$FC(NF_2)_3$	16.45 ± 0.20	48,300 ± 600
$F_2C(NF_2)_2$	15.75 ± 0.17	53,600 ± 400

Influence of Additives upon the Pyrolysis Rates. The first-order rate constants for the thermal decomposition of $FC(NF_2)_3$ were found to be unaffected by the addition of relatively high concentrations of N_2F_4, F_2, O_2, N_2O_4, or NO.[14] In these experiments, the ratios of additive concentration to $FC(NF_2)_3$ concentration were, respectively, 1.2, 0.6, 0.1, 0.8, and 0.4. The lack of effect of N_2F_4, which is completely dissociated to NF_2 radicals at reaction temperature,[15] indicates that NF_2 does not abstract F atoms from $FC(NF_2)_3$. It was also found that the addition of the less stable $FC(NF_2)_3$ to $F_2C(NF_2)_2$ does not affect the decomposition rate of $F_2C(NF_2)_2$.

Homogeneity of Decomposition. Four factors indicate that a heterogeneous component was not contributing to the rate-determining process in the thermal decompositions of these species. (1) The rates were unaffected by continued passivation of the reactors over a period of several months. (2) The observed Arrhenius parameters are higher than normally expected for a heterogeneous reaction.[16] (3) The rates of $C(NF_2)_4$ decomposition were the same in Teflon-coated and uncoated static reactors and were in agreement with the rates obtained in the stirred flow reactor. (4) The rate of $FC(NF_2)_3$ pyrolysis was the same in tubular and stirred flow reactors even though the S/V ratio of the former was eight times that of the latter.

Bond Dissociation Energies. All available data suggest that the initial and rate-determining step in each of these decompositions involves the rupture of a C–N bond

$$F_xC(NF_2)_{4-x} \longrightarrow F_x\dot{C}(NF_2)_{3-x} + \cdot NF_2 \qquad (5)$$

Because the reverse of eq 5 would be expected to have close to zero activation energy, the measured activation energies (Table II) for the decomposition of $C(NF_2)_4$, $FC(NF_2)_3$, and $F_2C(NF_2)_2$ yield a direct measure of the bond dissociation energy for the first C–N bond in each of these molecules. These activation energies are plotted in Figure 5. It may be seen that linear extrapolation to the next member of the series, CF_3NF_2,

(14) The experimental data have been deposited as Document No. NAPS-00898 with the ASIS National Auxiliary Publication Service, c/o CCM Information Corp., 909 3rd Ave., New York, N.Y. 10022. Remit $1.00 for microfiche or $3.00 for photocopies payable to CCMIC-NAPS.

(15) "JANAF Thermochemistry Tables," Dow Chemical Co., Midland, Mich.

(16) J. M. Thomas and W. J. Thomas, "Introduction to the Principles of Heterogeneous Catalysis," Academic Press, New York, 1967, p 55.

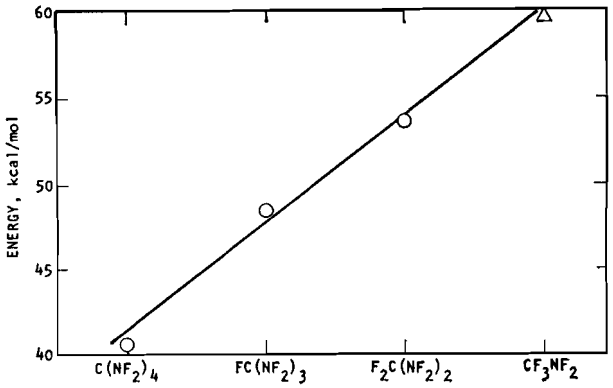


Figure 5. Comparison of activation energies for $C(NF_2)_4$, $FC(NF_2)_3$, and $F_2C(NF_2)_2$ with the bond dissociation energy of CF_3NF_2.

would predict a C–N bond of about 60 kcal/mol. The C–N bond in CF_3NF_2 measured by the electron impact technique[17] is 59.7 as shown in Figure 5. It appears, therefore, that the replacement of an NF_2 group by an F atom increases the bond dissociation energy for the first C–N bond by about 6.3 kcal/mol.[18] This explains the marked differences in the thermal stabilities of these compounds.

Products of Pyrolysis

Product Distribution as a Function of Residence Time. The product distributions from the species $C(NF_2)_4$, $FC(NF_2)_3$, and $F_2C(NF_2)_2$ at 224, 339, and 424°, respectively, are presented in Figures 6, 7, and 8 as a function of residence time. In these initial experiments, gas chromatographic calibration factors were not measured, and column *C* was employed which did not separate N_2, CF_4, and NF_3 (Table I). Therefore, the concentration of each entity is indicated by its gas chromatographic peak area. Hence, although Figures 6, 7, and 8 show the effect of residence time on product distribution, they give only approximate indications of the relative concentrations of the various species. In subsequent experiments, calibration factors were determined and columns were developed to separate N_2, CF_4, and NF_3. It was found that all three are major products from each of these reactions. The analytical techniques employed in this investigation were not capable of detecting F_2; it is possible that F_2 also is a product.

Products from $C(NF_2)_4$. It may be seen from Figure 6 that the concentrations of the species N_2, NF_3, CF_4, and CF_3NF_2 rise continuously with residence time in a manner indicating that they are stable products. The compounds $(NF_2)_2C{=}NF$, $F(NF_2)C{=}NF$, $F_2C{=}NF$, and N_2F_4 rise to a maximum and then decrease in a manner indicating that they are either thermally unstable products or are reaction intermediates (*i.e.*, react with radicals or other molecules formed in the pyrolysis). Throughout this paper, these species will be referred to as "intermediates."

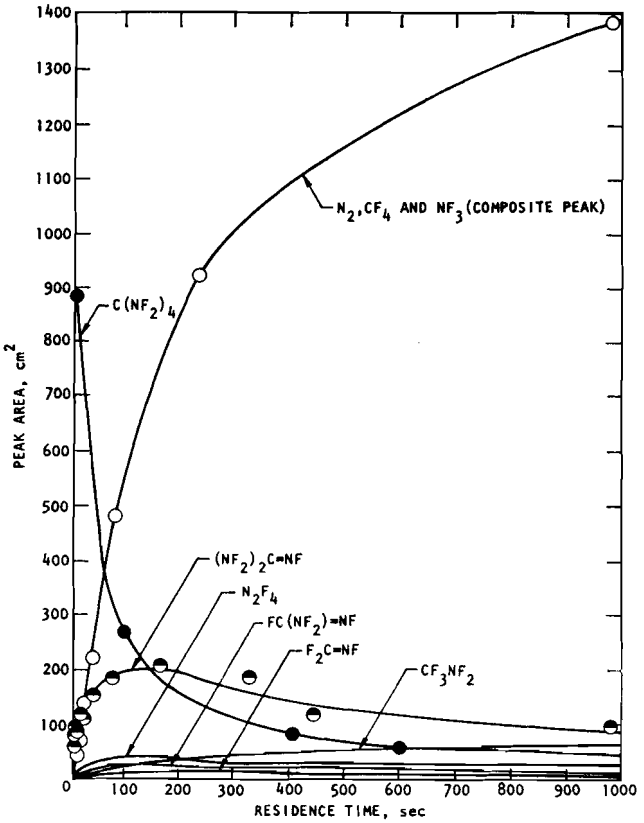


Figure 6. Product distribution from $C(NF_2)_4$ as a function of residence time at 224°.

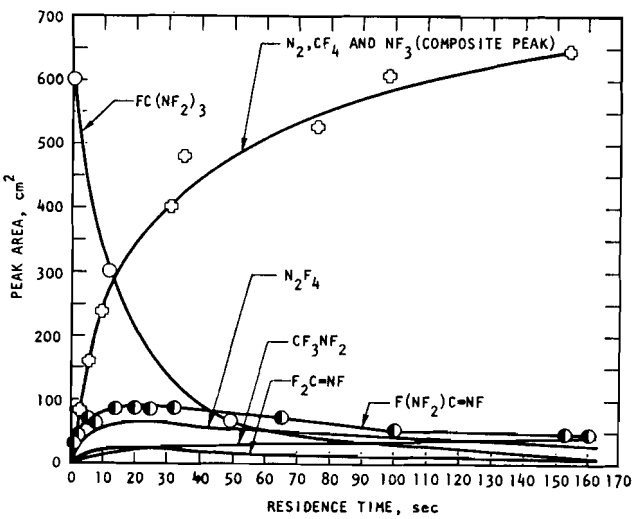


Figure 7. Product distribution from $FC(NF_2)_3$ as a function of residence time at 339°.

Neither $FC(NF_2)_3$ nor $F_2C(NF_2)_2$ was detected as a product of this reaction, even though both of these species are thermally more stable (Figure 4) than $C(NF_2)_4$. This has important implications in the mechanism that we propose.

(17) Unpublished results from Rohm and Haas Co.

(18) Nazin, *et al.*,[7] found that the replacement of NO_2 by F increased D(C–N) by 4–6 kcal/mol in the polynitrofluoroalkanes.

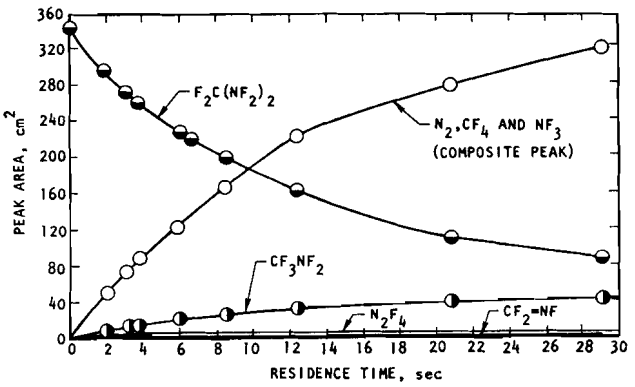


Figure 8. Product distribution from $F_2C(NF_2)_2$ as a function of residence time at 424°.

Products from $FC(NF_2)_3$. The products from $FC(NF_2)_3$ at 339°, presented in Figure 7, are identical with those from $C(NF_2)_4$ except for the absence of $(NF_2)_2C{=}NF$. The stable products are N_2, NF_3, CF_4, and CF_3NF_2 (minor product), while the intermediates are $F(NF_2)C{=}NF$, $F_2C{=}NF$, and N_2F_4. The behavior of the intermediates with residence time is quite analogous to the $C(NF_2)_4$ case. It was definitely established that $F_2C(NF_2)_2$ is not present either as an intermediate or product. $F_2C(NF_2)_2$ is more stable than $FC(NF_2)_3$, and it was shown that the addition of $FC(NF_2)_3$ did not influence the rate of $F_2C(NF_2)_2$ decomposition. Thus, if $F_2C(NF_2)_2$ were formed, it would have been detected.

Products from $F_2C(NF_2)_2$. As seen from Figure 8, the products from $F_2C(NF_2)_2$ at 424° are identical with those from $FC(NF_2)_3$ except for the absence of $F(NF_2)$-$C{=}NF$. The products are N_2, CF_4, NF_3, and CF_3NF_2 (minor product), while the intermediates are $F_2C{=}NF$ and N_2F_4. N_2 is a major product from $F_2C(NF_2)_2$ even though the radicals formed during the initial C–N bond rupture contain only one N atom.

Product Distribution at Short Residence Times. In the case of $C(NF_2)_4$ and $FC(NF_2)_3$, considerable information is obtained by examining the product distribution at the shortest residence times employed.

For $C(NF_2)_4$ at 224° the shortest residence time was 4.0 sec. The integrated peak areas (in arbitrary units) for the products and intermediates were $(NF_2)_2C{=}NF$, 50; N_2, CF_4, NF_3 composite, 36; N_2F_4, 6.0; $F(NF_2)C{=}NF$, 3.3; CF_3NF_2, 3.3; and $F_2C{=}NF$, 0. Hence the most abundant species is the double-bonded intermediate $(NF_2)_2C{=}NF$.[19] At this short residence time, the amount of $(NF_2)_2C{=}NF$ in the products is approximately 70% of the $C(NF_2)_4$ which has decomposed.

For $FC(NF_2)_3$ at 339°, the shortest residence time was 0.51 sec. The peak areas were $F(NF_2)C{=}NF$, 20.5; N_2, CF_4, NF_3 composite, 18.4; N_2F_4, 8.3; $F_2C{=}NF$, 2.0; and CF_3NF_2, 0.8. Again, the major species is the corresponding double-bonded intermediate $F(NF_2)C{=}NF$. Approximately 50% of the $FC(NF_2)_3$ which decomposes is recovered as $F(NF_2)C{=}NF$.

At longer residence times the moles of $(NF_2)_2C{=}NF$ and $F(NF_2)C{=}NF$, respectively, recovered per mole of $C(NF_2)_4$ and $FC(NF_2)_3$ decomposed become progressively less (see Figures 6 and 7). The results at short residence times indicate that the formation of the double-bonded intermediates, $(NF_2)_2C{=}NF$ and $F(NF_2)C{=}NF$, is a major initial process in thermal decomposition of $C(NF_2)_4$ and $FC(NF_2)_3$, respectively.

Thermal Stability of N_2F_4. In Figures 6, 7, and 8 the concentration of N_2F_4 is seen to rise to a maximum and then decrease at longer residence times.

The thermal stability of N_2F_4 was measured in the stirred flow reactor to determine whether this behavior might be attributed to thermal instability of N_2F_4. It is recognized, of course, that at these temperatures N_2F_4 is almost completely dissociated to NF_2 radicals, but these radicals recombine to N_2F_4 before reaching the chromatographic column. When an N_2F_4–Hel mixture was passed through the heated reactor, decomposition occurred at temperatures above 550°, but the results were very erratic and nonreproducible indicating a heterogeneous reaction. However, these experiments did demonstrate that N_2F_4 does not decompose at a measurable rate below 550°. Hence, the behavior of N_2F_4 in Figures 6, 7, and 8 cannot be attributed to thermal instability.

Variation of Products and Intermediates with Temperature. The temperature dependence of the yield of the principal intermediates, $(NF_2)_2C{=}NF$ from $C(NF_2)_4$ and $F(NF_2)C{=}NF$ from $FC(NF_2)_3$, was investigated to establish the role of these species in the decomposition mechanism.

Figure 9 shows plots of $(NF_2)_2C{=}NF$ concentration *vs.* per cent $C(NF_2)_4$ decomposed at 198 and 250° for the same initial concentration of $C(NF_2)_4$. These results clearly demonstrate that the observed $(NF_2)_2C{=}NF$ concentrations are strongly temperature dependent, with much more $(NF_2)_2C{=}NF$ being formed at 250 than at 198°. Also, the residence time at which the maximum concentration occurs is shifted to lower per cent decomposition at the lower temperature. At 198°, the maximum occurs at about 17% reaction, while at 250° the maximum occurs at about 59% reaction.

Very similar behavior was observed in the case of $FC(NF_2)_3$ decomposition. Figure 10 gives similar plots for $F(NF_2)C{=}NF$ from $FC(NF_2)_3$ at 303 and 355°. Again, the observed concentration of the principal intermediate is seen to be very strongly temperature dependent. Similary to $C(NF_2)_4$, the maximum concentration occurs at about 18% decomposition at 303°, while at 355° the maximum is shifted to about 70% reaction.

(19) Although the gas chromatographic peak area for $(NF_2)_2C{=}NF$ is larger than for the composite N_2, CF_4, NF_3 peak, the total concentration of N_2, CF_4, and NF_3 is actually higher than $(NF_2)_2C{=}NF$ because the calibration factors, F_i, are higher for the lower molecular weight species.

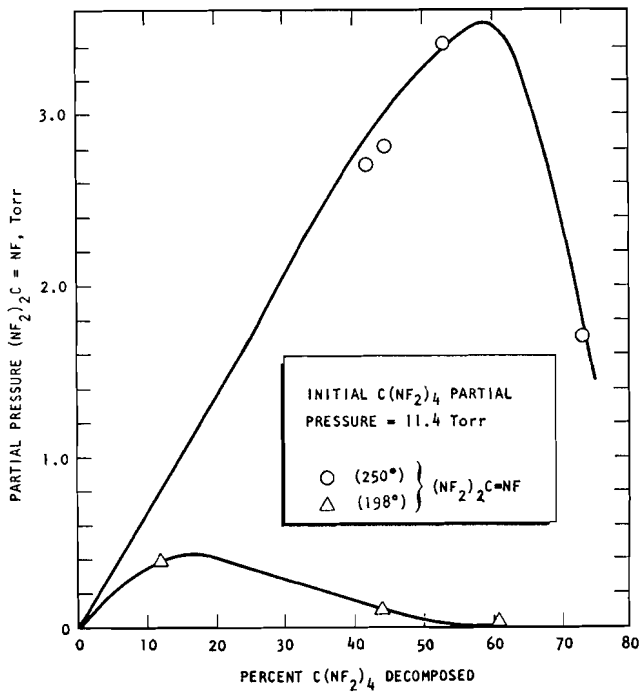


Figure 9. Influence of temperature on formation of $(NF_2)_2C=NF$ from $C(NF_2)_4$.

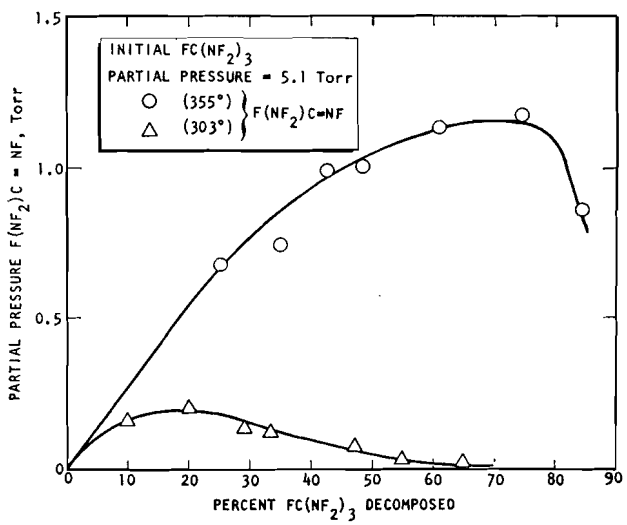


Figure 10. Influence of temperature on formation of $F(NF_2)C=NF$ from $FC(NF_2)_3$.

These results suggest that stable product formation from $FC(NF_2)_3$ should be retarded initially at higher temperatures, because of the increased formation of the principal intermediate, $F(NF_2)C=NF$. That this is indeed the case may be seen by comparing Figures 11 and 12 in which the concentrations of N_2, NF_3, and CF_4 as a function of residence time at 322 and 354°, respectively, are plotted. As seen, higher concentrations of N_2, NF_3, and CF_4 are formed initially per mole of $FC(NF_2)_3$ decomposed at the lower temperature. For example, at 50% decomposition, one-half as much N_2 is formed at 354 as at 322°.

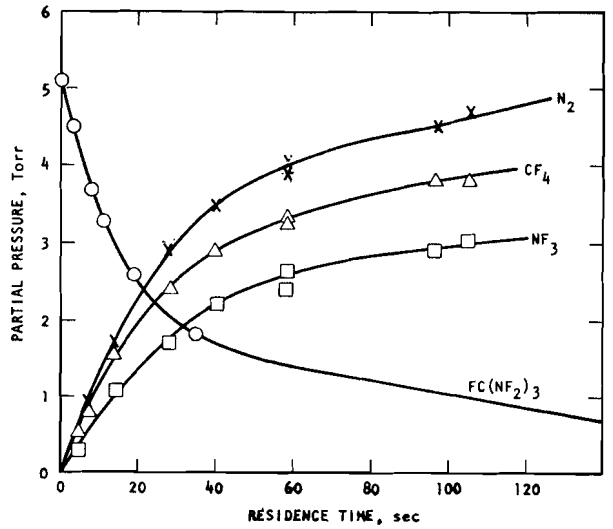


Figure 11. Formation of N_2, NF_3, and CF_4 from $FC(NF_2)_3$ at 322°.

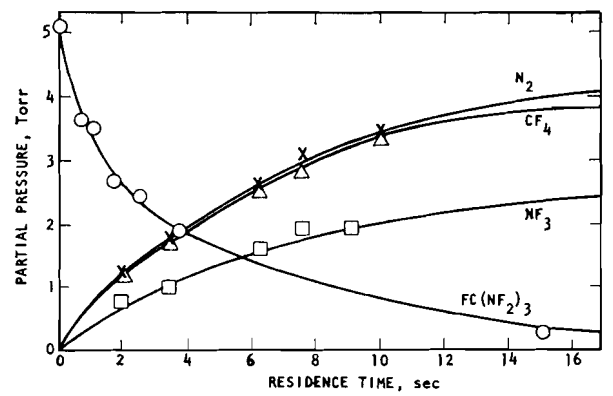


Figure 12. Formation of N_2, NF_3, and CF_4 from $FC(NF_2)_3$ at 354°.

In view of the above results, it appeared of interest to investigate the decomposition of $C(NF_2)_4$ at much higher temperatures and consequently much shorter residence times than were obtainable in the 90-ml stirred flow reactor. For this purpose, the small 2.4-ml tubular reactor was employed.

The results of a series of experiments conducted at 344° and residence times from 7 to 190 msec are presented in Figure 13. $C(NF_2)_4$ is more than 99% decomposed at residence times above approximately 60 msec. The principal products under these conditions are $(NF_2)_2C=NF$, NF_3, and N_2F_4. In agreement with the trend in Figure 9, the concentration of $(NF_2)_2C=NF$ reaches approximately 85% of the initial $C(NF_2)_4$ concentration at this higher temperature and then begins to decompose slowly at longer residence times.

It would appear from Figure 13 that the species present at the second highest concentration is NF_3. It should be noted, however, that N_2F_4 is completely dissociated into NF_2 at this temperature and partial pressure. Thus, the concentration of NF_2 radicals in

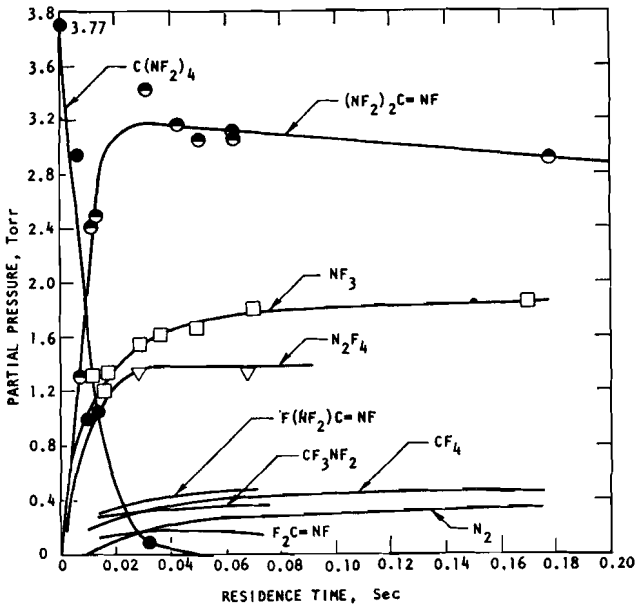


Figure 13. Product distribution from $C(NF_2)_4$ as a function of residence time at 344°.

the reactor is actually greater than that of NF_3. Smaller amounts of $F(NF_2)C{=}NF$, $F_2C{=}NF$, CF_3NF_2, CF_4, and N_2 are also formed under these conditions.

Kinetic Model

Because of the complexity of the products and intermediates which form after the initial C–N bond rupture, additional experiments were required to establish the exact nature of the secondary processes that occur. These results and the overall kinetic processes will be discussed before discussing the mechanism of the individual reactions.

The high concentrations of NF_2 at short residence times is very strong evidence that the initial and rate-determining step in the thermal decompositions of $C(NF_2)_4$, $FC(NF_2)_3$, and $F_2C(NF_2)_2$ is the simple rupture of the C–N bond. The influence of temperature upon the principal intermediates $(NF_2)_2C{=}NF$ and $F(NF_2)C{=}NF$ (Figures 9 and 10) and the results presented in Figure 13 are in agreement with a kinetic model in which it is assumed that $C(NF_2)_4$ and $FC(NF_2)_3$ decompose by the following overall processes

$$C(NF_2)_4 \xrightarrow{\text{I}} (NF_2)_2C{=}NF + xNF_2 + (1-x)NF_3 + xF \xrightarrow{\text{II}} \text{products} \quad (6a)$$

$$FC(NF_2)_3 \xrightarrow{\text{I}} F(NF_2)C{=}NF + xNF_2 + (1-x)NF_3 + xF \xrightarrow{\text{II}} \text{products} \quad (6b)$$

where the processes leading to products, step II, have lower activation energies than the rate-determining process in step I (C–N bond rupture). Thus, higher maximum yields of $(NF_2)_2C{=}NF$ and $F(NF_2)C{=}NF$ are obtained at higher temperatures.

The processes by which $(NF_2)_2C{=}NF$ or $F(NF_2)C{=}NF$ react to form stable products and other intermediates in the above model for the decomposition of $C(NF_2)_4$ and $FC(NF_2)_3$, respectively (step II of eq 6), were investigated by first assuming that $(NF_2)_2C{=}NF$ and $F(NF_2)C{=}NF$ disappear solely by thermal decomposition. To determine if this were a valid assumption, the thermal decompositions of $(NF_2)_2C{=}NF$ and $F(NF_2)C{=}NF$ were investigated in the stirred flow reactor.[20] The following calculations were made to test this assumption.

Assuming the kinetic model shown in eq 6, the observed maximum concentrations of the principal intermediate (Figures 9, 10, and 13) can be put on a more quantitative basis. Equation 6 can be written

$$A \xrightarrow{k_a} B \xrightarrow{k_b} \text{products} \quad (7)$$

where A and B are the concentrations of the reactant and principal double-bonded intermediate, respectively. If it is assumed that B decomposes by a first-order process, then for a stirred flow reactor

$$dB/dt = k_aA - k_bB - B/\tau = 0 \quad (8)$$

The residence time at which B reaches a maximum, τ_{max}, can be obtained by differentiating eq 8 after substituting for A from eq 2. This gives

$$\tau_{max} = (k_ak_b)^{-1/2} \quad (9)$$

From eq 2, the percentage of A decomposed is given by $P = 100k_a(1 + k_a\tau)^{-1}$. Therefore, P_{max}, which is the percentage of A reacted at maximum B, is given by

$$P_{max} = 100[1 + (k_b/k_a)^{1/2}]^{-1} \quad (10)$$

The form of eq 10 is in agreement with the experimentally observed shifting of the maximum concentrations of the principal intermediates to higher per cent reaction at higher temperatures (Figure 9).

On the basis of eq 8, it is possible to predict the maximum yield of $(NF_2)_2C{=}NF$, B_{max}/A_0, as a function of temperature, assuming still that $(NF_2)_2C{=}NF$ is

Table III: Formation of $(NF_2)_2C{=}NF$ from $C(NF_2)_4$ as a Function of Temperature

Temp, °C	τ_{max}, sec		P_{max}, %		B_{max}/A_0	
	Obsd	Calcd	Obsd	Calcd	Obsd	Calcd
198	180	260	19	39	0.04	0.15
250	7	17	58	73	0.26	0.54

(20) A. E. Axworthy and J. M. Sullivan, *J. Phys. Chem.*, in preparation. The kinetics and mechanism of the decomposition of $(NF_2)_2C{=}NF$ and $F(NF_2)C{=}NF$ will be reported. $(NF_2)_2C{=}NF$ decomposition is apparently heterogeneous over the temperature range 210 to 323° with $k_1 = 10^{3.5}\exp(-12{,}360/RT)$ sec^{-1}. The decomposition products from $(NF_2)_2C{=}NF$ are $F(NF_2)C{=}NF$, $F_2C{=}NF$, CF_3NF_2, N_2, CF_4 and small amounts of N_2F_4 and NF_3. The products from $F(NF_2)C{=}NF$ are $F_2C{=}NF$, CF_3NF_2, N_2, and CF_4.

Table IV: Influence of Additives on the Intermediate and Products Formed during the Thermal Decomposition of $FC(NF_2)_3$

Temp, °C	τ, sec	Partial pressure of $FC(NF_2)_3$, Torr	Additive	Additive partial pressure, Torr	Peak area: CF_3NF_2	$F_2C{=}NF$	N_2F_4	$F(NF_2)C{=}NF$	N_2, NF_3, CF_3 composite
339.5	57.1	4	None	0	17.5	6.1	22.9	29.1	238
340.3	53.9	4	None	0	16.9	6.1	24.0	32.8	254
340.1	54.1	4	N_2F_4	6	19.8	19.8	...	62.1	280
340.1	54.8	4	N_2F_4	6	18.0	17.6	...	57.2	286
339.9	55.9	4	None	0	17.0	7.3	24.0	37.7	258
339.3	11.8	1.5	None	0	9.1	8.3	11.5	44.6	151
339.5	11.9	1.5	None	0	9.4	9.0	11.7	42.7	152
339.5	12.0	1.5	F_2	1.3	12.1	2.4	2.2	25.0	240
339.1	11.9	1.5	F_2	1.3	17.3	3.5	2.6	17.1	270

consumed only by pyrolysis. From eq 8, the ratio of $(NF_2)_2C{=}NF$ to $C(NF_2)_4$ is given by

$$B/A = k_a(k_b + 1/\tau)^{-1} \quad (11)$$

Thus, the ratio of $(NF_2)_2C{=}NF$ concentration to initial $C(NF_2)_4$ concentration is given by

$$B/A_0 = k_aA[(k_b + 1/\tau)A_0]^{-1} \quad (12)$$

The calculated and observed values (Figure 9) of τ_{max}, P_{max}, and B_{max}/A_0 for the formation of $(NF_2)_2C{=}NF$ from $C(NF_2)_4$ are presented in Table III as a function of temperature. It may seen that the trend with temperature is that which would be predicted by a kinetic model, eq 6, in which each molecule of $C(NF_2)_4$ forms one molecule of $(NF_2)_2C{=}NF$ which then decomposes (heterogeneously). However, the observed values of τ_{max}, P_{max}, and B_{max}/A_0 in Table III are all smaller than the predicted values indicating that $(NF_2)_2C{=}NF$ also reacts by processes other than simple thermal decomposition.[21]

Application of the above model to the decomposition of $FC(NF_2)_3$ results in even greater discrepancies between the observed and calculated quantities. $F(NF_2)C{=}NF$ is sufficiently stable[20] that very high yields of this intermediate should be obtained from $FC(NF_2)_3$. That this is not the case (Figure 10) again indicates the predominance of processes other than thermal decomposition.

The most likely processes for the consumption of $(NF_2)_2C{=}NF$ and $F(NF_2)C{=}NF$ are reactions with NF_2 or F atoms. For this reason, experiments were conducted to determine the influence of added NF_2 and F_2 on the concentrations of $(NF_2)_2C{=}NF$ and $F(NF_2)C{=}NF$ formed from $C(NF_2)_4$ and $FC(NF_2)_3$, respectively. It was reported above that these additives do not alter the decomposition rate of $FC(NF_2)_3$. It was found[14] that the addition of N_2F_4 at a concentration of 4.5 Torr increased by about 25% the concentration of $(NF_2)_2C{=}NF$ formed from $C(NF_2)_4$ (at 240°, τ = 9 sec, and $C(NF_2)_4$ = 6 Torr). The influence of added N_2F_4 and F_2 on the product distribution from $FC(NF_2)_3$ at 340° is shown in Table IV. Addition of N_2F_4 (τ = 55 sec) causes a twofold increase in $F(NF_2)C{=}NF$ concentration, while the addition of F_2 (τ = 12 sec) decreases the concentrations of $F(NF_2)C{=}NF$ and N_2F_4 by factors of about 2 and 4, respectively.

The results of these experiments suggest that F atoms formed in the initial decomposition process attack the principal intermediates $(NF_2)_2C{=}NF$ and $F(NF_2)C{=}NF$, while NF_2 promotes their longevity by itself reacting with fluorine to form NF_3. That this is apparently the case is demonstrated by the data in Table V, which shows the influence of N_2F_4 on the peak areas for N_2, CF_4, and NF_3 formed from $FC(NF_2)_3$ at 323° and residence times of about 4 sec. The addition of N_2F_4 is seen to increase the concentration of NF_3 by more than a factor of 2.

Table V: Influence of N_2F_4 on Formation of N_2, NF_3, and CF_4 from $FC(NF_2)_3$ at 323°

U, ml/sec	τ, sec	Partial pressure $FC(NF_2)_3$, Torr	Partial pressure N_2F_4, Torr	Peak area: N_2	CF_4	NF_3
2.20	4.19	3.5	0	107	158	75
2.24	4.11	3.6	0	106	156	77
2.30	4.01	3.5	3.8	116	136	163
2.28	4.04	3.7	3.5	114	148	166

The products[20] from the pyrolyses of $(NF_2)_2C{=}NF$ and $F(NF_2)C{=}NF$ are the same as those from $C(NF_2)_4$ and $FC(NF_2)_3$, respectively, except that higher yields of N_2F_4 and NF_3 are obtained from $C(NF_2)_4$ and $FC(NF_2)_3$. It appears, therefore, that $(NF_2)_2C{=}NF$ and $F(NF_2)C{=}NF$ each yield essentially the same products whether

(21) A similar calculation can be made for the tubular reactor data at 344° in Figure 13 [S. W. Benson, "The Foundations of Chemical Kinetics," McGraw-Hill, New York, N. Y., 1960, p 34]. The decomposition rate of $(NF_2)_2C{=}NF$ was not measured in this reactor, but an approximate k_b value of 0.6 sec^{-1} can be obtained from the final slope of the $(NF_2)_2C{=}NF$ curve in Figure 13. This gives a calculated value of B_{max}/A_0 of 0.96 *vs.* an observed value (Figure 13) of 0.84, indicating that more than one reaction path occurs for $(NF_2)_2C{=}NF$ even at this higher temperature (*i.e.*, approximately 10% reacts by processes other than pyrolysis).

decomposed thermally or by F atom attack. When $C(NF_2)_4$ and $(NF_2)_2C{=}NF$ were each pyrolyzed at 528° in the 2.4-ml tubular reactor, the same product distribution was obtained as a function of residence time, except for higher concentrations N_2F_4 and NF_3 from $C(NF_2)_4$; at this high temperature, nearly all of the $(NF_2)_2C{=}NF$ formed from $C(NF_2)_4$ should decompose thermally.

Mechanism

The formation of N_2F_4 and $(NF_2)_2C{=}NF$ as initial decomposition products is strong evidence that the initial step in $C(NF_2)_4$ pyrolysis is the cleavage of a C–N bond

$$C(NF_2)_4 \longrightarrow \cdot C(NF_2)_3 + NF_2 \qquad (13)$$

followed by the first or both of the following processes

$$\cdot C(NF_2)_3 \longrightarrow (NF_2)_2C{=}NF + F \qquad (14)$$

$$\cdot C(NF_2)_3 + NF_2 \longrightarrow (NF_2)_2C{=}NF + NF_3 \qquad (15)$$

The fact that the concentration of NF_3 is less than that of $(NF_2)_2C{=}NF$ (Figure 13) indicates that reaction 15 is not the predominant process. Reaction 14 is apparently so rapid that no other process can compete, including the reverse of reaction 13 which would lead to inhibition by added N_2F_4. Much or all of the NF_3 probably results from reaction of NF_2 radicals with fluorine atoms generated in reaction 14.

$$NF_2 + F + M \longrightarrow NF_3 + M \qquad (16)$$

According to the proposed kinetic model, the remainder of the products—N_2, CF_4, CF_3NF_2, $F(NF_2)C{=}NF$, and $F_2C{=}NF$—are formed from reactions of the primary intermediate $(NF_2)_2C{=}NF$. Reactions analogous to eq 13, 14, and 15 are proposed for $FC(NF_2)_3$ decomposition. Although the data are sparse in the case of $F_2C(NF_2)_2$, the similarity of its product distribution (Figure 8) with those for $C(NF_2)_4$ and $FC(NF_2)_3$ (Figures 6 and 7) suggests that the mechanism is similar.

The absence of chain processes in this system of compounds is of particular interest. The experimental observation that NF_2 does not influence the rate of decomposition and that $FC(NF_2)_3$ is not a product of $C(NF_2)_4$ pyrolysis indicates that reactions such as eq

$$\cdot NF_2 + C(NF_2)_4 \longrightarrow (\cdot NF)C(NF_2)_3 + NF_3 \qquad (17)$$

$$\cdot C(NF_2)_3 + C(NF_2)_4 \longrightarrow FC(NF_2)_3 + (\cdot NF)C(NF_2)_3 \qquad (18)$$

17 and 18 do not occur. Benson[22] has pointed out that reactions such as eq 17 involving fluorine abstraction are likely to have prohibitively high activation energies; this accounts for the nonchain character of these reactions.

(22) Reference 9, p 122.